ACS OMEGA

http://pubs.acs.org/journal/acsodf

Article

Biosynthesis of Silver Nanoparticles Using *Cucumis prophetarum* Aqueous Leaf Extract and Their Antibacterial and Antiproliferative Activity Against Cancer Cell Lines

Hemlata, Prem Raj Meena, Arvind Pratap Singh, and Kiran Kumar Tejavath*

Cite This: *ACS Omega* 2020, 5, 5520−5528

Read Online

ACCESS | Metrics & More | Article Recommendations

ABSTRACT: Biosynthesized nanoparticles are gaining attention because of biologically active plant secondary metabolites that help in green synthesis and also due to their unique biological applications. This study reports a facile, ecofriendly, reliable, and cost-effective synthesis of silver nanoparticles using the aqueous leaf extract of *Cucumis prophetarum* (*C. prophetarum*) and their antibacterial and antiproliferative activity. Silver nanoparticles were biosynthesized using the aqueous leaf extract of *C. prophetarum*, which acted as a reducing and capping agent. The biosynthesized *C. prophetarum* silver nanoparticles (Cp-AgNPs) were characterized using different techniques, such as UV−visible spectroscopy, dynamic light scattering (DLS), Fourier transform infrared (FTIR) spectroscopy, X-ray diffraction (XRD), scanning electron microscopy (SEM) and energy-dispersive X-ray analysis (EDAX). Phytochemical analysis was performed to determine the phytochemicals responsible for the reduction and capping of the biosynthesized Cp-AgNPs. The antioxidant activity of the biosynthesized nanoparticles was determined using 2,2-diphenyl-1-picrylhydrazyl (DPPH) and 3-ethylbenzothiazoline-6-sulfonic acid (ABTS) assays. Their antibacterial activity was checked against *Staphylococcus aureus* (Gram-positive) and *Salmonella typhi* (Gram-negative) bacteria. The biosynthesized nanoparticles showed dosage-dependent inhibition activity with a significant zone of inhibition and were more effective toward *S. typhi* as compared to *S. aureus*. Their antiproliferative activity was evaluated using 3-(4,5-dimethylthiazol-2-yl)-2,5-diphenyltetrazolium bromide (MTT) assay on selected cancer cell lines. The IC_{50} values of Cp-AgNPs on A549, MDA-MB-231, HepG2, and MCF-7 were found to be 105.8, 81.1, 94.2, and 65.6 μg/mL, respectively, and this showed that the Cp-AgNPs were more potent toward MCF-7 as compared to other cell lines used in this study. This work revealed that the biosynthesized silver nanoparticles using *C. prophetarum* leaf extract were associated with good antibacterial activity and antiproliferative potential against selected cancer cell lines. The biosynthesized *C. prophetarum* AgNPs can be further exploited as a potential candidate for antioxidant, antibacterial, and anticancer agents.

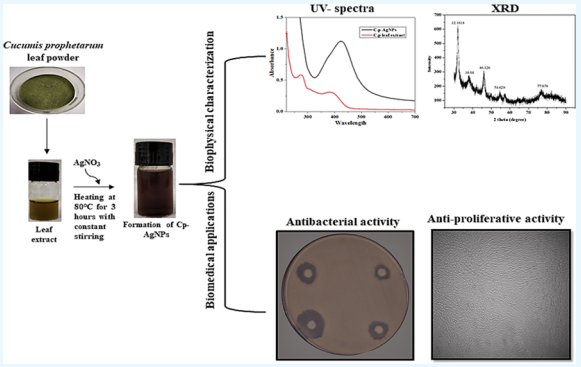

INTRODUCTION

Nanotechnology has emerged as one of the large and attractive areas of research, offering unique features and extensive applications in various sectors such as agriculture, food, and biomedicine.[1] Properties associated with nanoparticles such as their small size, large surface area to surface volume ratio, optical, magnetic, chemical, and mechanical properties have made them candidates for novel applications in the biomedical field as antibiotic, antioxidant, and anticancer agents and are well documented.[2] Nanoparticles of noble metals, such as silver, gold, platinum, copper, zinc, titanium, and magnesium, have gained considerable attention for biomedical applications due to their multifunctional theranostic abilities.[3] Even though chemical and physical methods are employed in the synthesis of nanoparticles, they are associated with hazardous chemicals exhibiting toxicity. Alternatively, plant-mediated synthesis of metal nanoparticles is gaining attention because of the low toxicity, cost effectiveness, ecofriendliness, and low time consumption.[4] Further, plants are a good and easily available source of bioactive plant secondary metabolites such as polysaccharides, proteins, polyphenols, flavonoids, terpenoids, tannins, alkaloids, amines, ketones, and aldehydes, which act as reducing, stabilizing, and capping agents in the conversion of metal ions to metal nanoparticles, leading to the production of desirable nanoparticles with predefined characteristics.[5] Among various biosynthesized metal nanoparticles, silver nanoparticles (AgNPs) have emerged as the champion in the

Received: January 13, 2020
Accepted: February 20, 2020
Published: March 2, 2020

https://dx.doi.org/10.1021/acsomega.0c00155
ACS Omega 2020, 5, 5520−5528

last two decades due to their unique biological, chemical, and physical properties.[6] Although silver is toxic at higher concentrations, many studies have established that a lower concentration of $AgNO_3$ has higher chemical stability, catalytic activity, biocompatibility, and intrinsic therapeutic potential.[7] Silver nanoparticles are reported to have potential anticancer and antimicrobial activity.[8] In fact, the slow and regulated release of silver from silver nanoparticles is one of the most striking advantages of these nanoparticles when compared with bulk metals and their salts.[9] A combination of nanotechnology and traditional medicine is the mantra of the new-age bio-nanoformulations.

Many studies have been done on the green synthesis of AgNPs using leaves of plants, but biosynthesis of AgNPs using wild and indigenous species exhibiting potential anticancer activity and antibacterial activity has not been explored to a large extent. Cucurbitaceae are herbaceous plants accounting for nearly 125 genera and more than 960 species, which include *Cucurbita*, *Langenaria*, *Citrullus*, *Cucumis*, and *Momordica*. This family is predominantly distributed throughout the tropic and in temperate regions. Among the various plant families, the cucurbitaceae family ranks the highest for a number and percentage of species used as human food.[10] Cucurbitacins found in fruits exhibit potent anticancer activity against various cancer cell lines.[11] The diversity of cucurbitacin activities, especially differential cytotoxicity toward renal, brain, tumor, and melanoma cell lines, makes them potential species for further exploration.[12] With this background knowledge, we have selected *Cucumis prophetarum*, commonly known as wild gourd or wild cucumber, which is associated with potent medicinal properties. *N*-Trisaccharide isolated from the aqueous extract of *C. prophetarum* fruits is known to possess antioxidant, hepatoprotective, and antidiabetic properties.[13] Along the same line of study, we tried to explore the antibacterial and antiproliferative potential associated with the leaves of *C. prophetarum* and silver nanoformulations. This study highlights the potential use of the *cucurbitaceae* family species in combination with nanotechnology for various biomedical applications.

RESULTS AND DISCUSSION

This study investigated the biosynthesis of *C. prophetarum* silver nanoparticles (Cp-AgNPs) and evaluation of the antibacterial and antiproliferative potential of nanoparticles using the aqueous leaf extract of *C. prophetarum*.

Phytochemical Analysis. Various phytochemical constituents in the aqueous leaf extract of *C. prophetarum* responsible for the reduction and capping of silver nanoparticles are qualitatively analyzed. From the phytochemical screening of the *C. prophetarum* aqueous leaf extract, it was found to be a good source of secondary metabolites, as shown in Table 1. Phytochemical analysis of aqueous leaf extracts of *Cucumis sativus*[14] and *Cucumis Melo*[15] has been reported with similar phytoconstituents. These phytochemicals may be responsible for the reduction of silver and acting as a capping agent to prevent aggregation of and provide stability to the nanoparticles.[16] The majority of the phytochemicals extracted in polar solvents are polar in nature and play a significant role in the synthesis of nanoparticles.[17]

Characterization of Cp-AgNPs. As the aqueous leaf extract of *C. prophetarum* was added to silver nitrate solution, the color of the solution changed from pale yellow to reddish-brown after 3 h because of the process of reduction of Ag^+ to

Table 1. Qualitative Phytochemical Screening of Aqueous Leaf Extracts of *C. Prophetarum*[a]

phytoconstituents	aqueous leaf extract
tannins	+
flavonoids	−
alkaloids	+
triterpenoids	+
phenol	+
saponins	+

[a]+Presence; −Absence.

Ag° nanoparticles (Figure 1A), and this indicated the biosynthesis of Cp-AgNPs. UV−vis spectra of the Cp-AgNPs and the aqueous leaf extract give a sharp peak at 420 nm after 3 h incubation (Figure 1B). UV−visible spectroscopy is one of the most widely used techniques for structural characterization of nanoparticles. The presence of an absorbance peak at about 420 nm clearly indicates the formation of AgNPs in the solution due to surface plasmon resonance (SPR) electrons present on the nanoparticle surface.[18] The SPR pattern is dependent on the characteristics of the individual metal particles, such as size and shape, as well as the dielectric properties of the medium used for synthesis and the inter-nanoparticle coupling interactions. The intensity of the SPR band increased with reaction time, indicating the synthesis of the AgNPs.

The hydrodynamic particle size distribution, polydispersity index (PDI), and surface charge (ζ-potential) of the biosynthesized Cp-AgNPs were measured using the dynamic light scattering (DLS) technique. The nanoparticle samples were appropriately diluted to reduce the background scattering. The size distribution graph shows the average size of the synthesized Cp-AgNPs to be approximately 90 nm with a low polydispersity index of 0.3 (Figure 2A), and the ζ-potential was observed to be −36.7 mV (Figure 2B). The hydrodynamic size includes the hydration layer on the surface of AgNPs; thus, this size is generally larger than the size measured from scanning electron microscopy (SEM) images. Additionally, the phytochemicals in the leaf extract may contribute to the hydrodynamic size. A nanoparticle size value below 150 nm and PDI values around 0.3 are adequate for uptake by cells.[19] Different phytochemicals present in extracts are mainly responsible for the various particle sizes. A similar range of particle sizes was observed with silver nanoparticles synthesized using red apple fruit extract.[20] The higher the negative or positive ζ-potential, the higher the stability, the better the colloidal properties due to electrostatic repulsion, and the higher the dispersity.[21] The ζ-potential of Cp-AgNPs was negative, suggesting that negatively charged functional groups from the plant extract contribute to the colloidal stability of the AgNPs.[6]

Fourier transform infrared (FTIR) spectroscopy was used to identify the secondary metabolites involved in the reduction and capping of Cp-AgNPs. The FTIR spectrum of the *C. prophaterum* leaf extract showed major absorption peaks at 3327.42, 2927.3, 1565.55, 1355.18, 1043.27, 832.05, 602.14, and 539.4 cm^{-1} (Figure 3A, red). The FTIR spectrum of Cp-AgNPs showed major absorption peaks at 3309.15, 2927, 1602, 1075, and 538 cm^{-1}, which signify the presence of phytoconstituents that act as capping agents (Figure 3A, blue).

The FTIR spectra of the *C. prophaterum* leaf extract corresponding to Cp-AgNPs showed major and minor shifts

https://dx.doi.org/10.1021/acsomega.0c00155
ACS Omega 2020, 5, 5520−5528

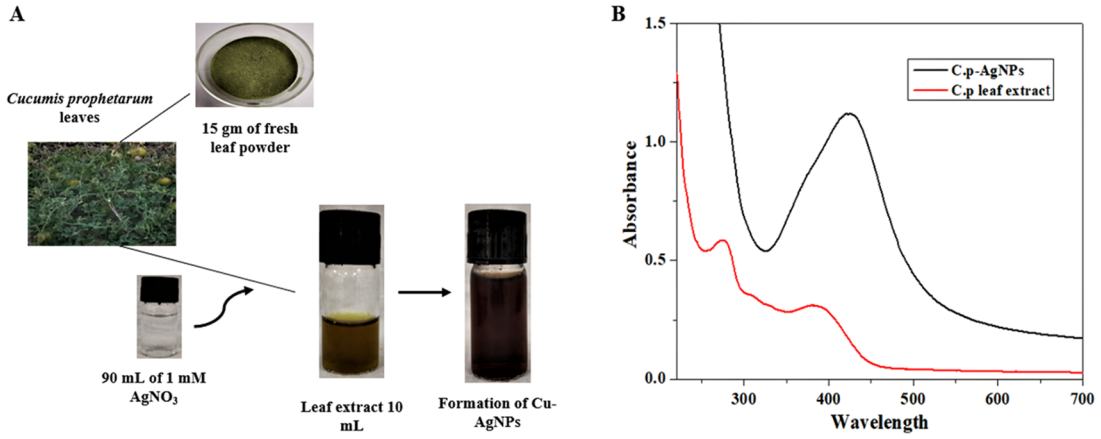

Figure 1. Biosynthesis of silver nanoparticles: (A) color change of the extract from pale yellow to dark brown after incubation at room temperature (RT); (B) UV spectra of the aqueous leaf extract and Cp-AgNPs synthesized from the *C. prophetarum* leaf extract.

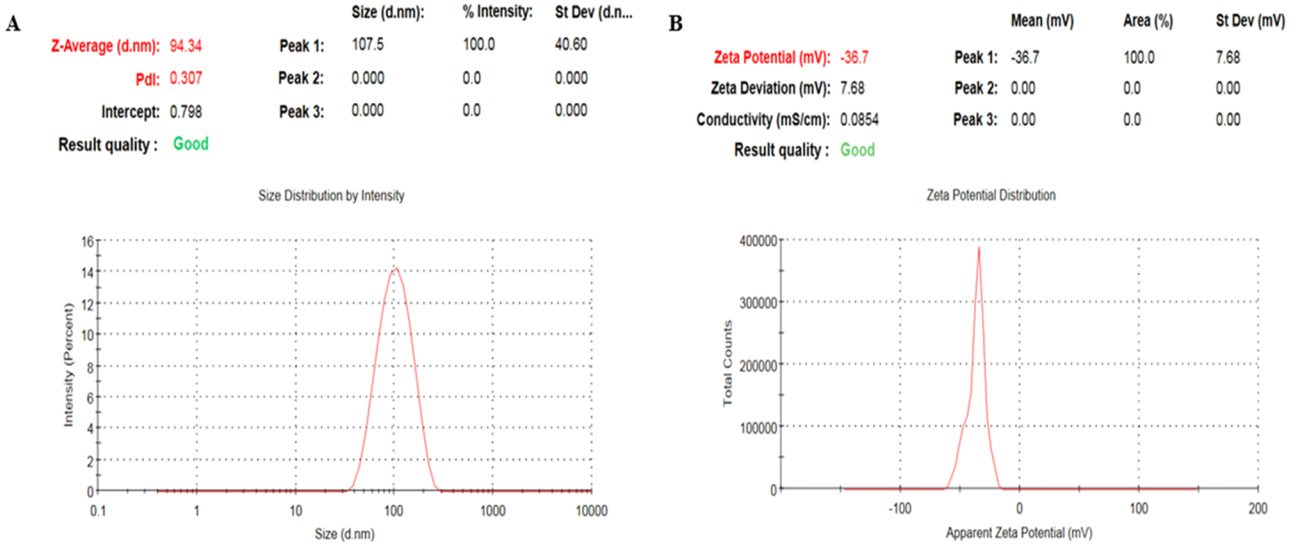

Figure 2. Nanoparticle size measurements: (A) size and PDI analysis; (B) ζ-potential of the biosynthesized Cp-AgNPs.

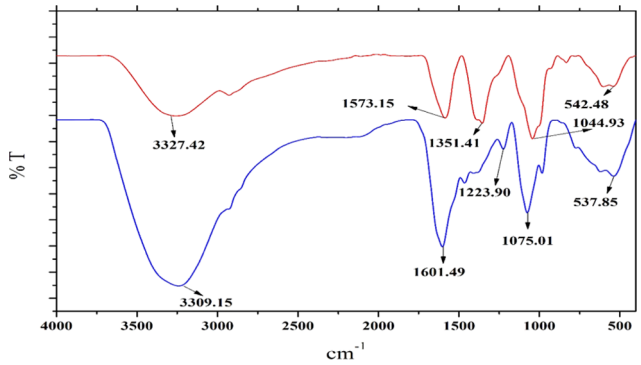

Figure 3. FTIR spectra of the *C. prophetarum* leaf extract (red) and Cp-AgNPs (blue) synthesized from the leaf extract.

of the peaks reasonably due to the reduction, capping, and stabilization of the synthesized nanoparticles.[22] A shift is observed for the peak at 3327.42 cm^{-1} to a lower wavelength of 3309.15 cm^{-1} due to the involvement of the O−H or N−H stretching of phenolic compounds that are present in the leaf extract;[23] the absorption peak at 2927.3 cm^{-1} is due to the C−H stretching of the methylene group or aliphatic group, and it is also a characteristic peak of triterpenoid saponins;[24] the band at 1565.55 cm^{-1} shifted to a higher wavelength 1602 cm^{-1} showing the involvement of alkenyl or aromatic C═C stretch; the band at 1355.18 cm^{-1} showed the presence of the −C−O stretching of phenol or tertiary alcohols; the band at 1043.27 cm^{-1} showed the O−H stretching of the phenol group;[25] the band at 832.05 cm^{-1} was because of the C−O stretch and C−S stretch or the involvement of aliphatic chloro compounds;[26] the band at 602.14 cm^{-1} might be due to the C−H stretching of the aromatic group; and the peak at 539.4 cm^{-1} showed the OH group of phenols. The majority of the peaks correspond to the phenolic groups of the polyphenols, triterpenoids, alkaloids, steroids, and tannins, adequately present in the leaf extract, which help in the formation of Cp-AgNPs.[27] These findings are inconsistent with the phytochemical analysis performed on the leaves of *C. prophaterum*.

The X-ray diffraction (XRD) pattern of the biosynthesized Cp-AgNPs shows five diffraction peaks at 2θ = 32.18, 38.04, 46.13, 54.63, and 77.08° (Figure 4). These major peaks in the spectrum, corresponding to the (111), (200), (120), (202), and (311) planes, respectively, reflect the patterns of the face-centered cubic (fcc) and crystalline structure of the

https://dx.doi.org/10.1021/acsomega.0c00155
ACS Omega 2020, 5, 5520−5528

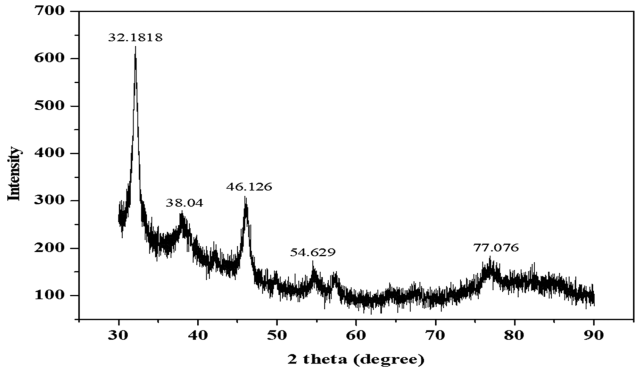

Figure 4. XRD pattern of the synthesized Cp-AgNPs using *C. prophetarum* leaf extract.

biosynthesized AgNPs. The peaks of the (111), (200), and (311) planes were also observed in the biosynthesized AgNPs using *Convolvulus arvensis* extract.[28] In addition, the peak of (120) was coincident with that of the AgNPs synthesized from *Excoecaria agallocha*.[29] The size of the nanoparticles will significantly influence the XRD peak patterns.[30] The presence of various reducing agents in the extract is responsible for the stabilization of AgNPs and, thus, for providing the crystalline structure of AgNPs, which was well studied in various biosynthesized nanoparticles.[31]

The morphology of the green-synthesized Cp-AgNPs was examined using SEM. The prepared Cp-AgNPs were found to be in polymorphic shapes; some of them were irregularly granulated, ellipsoidal, and highly aggregated, as shown in Figure 5A. Similar results were observed in the biosynthesis of silver nanoparticles using *Taraxacum officinale*.[32] The size of Cp-AgNPs from SEM analysis was found to be in the range of 30−50 nm (Figure 5A). Elemental analysis by EDX results showed a strong absorption peak of silver at 3 keV, which is due to silver being the major constituent[33] (Figure 5B). Microscopic analysis using a scanning electron microscope showed that the Cp-AgNPs were uniformly distributed and also showed that the formed nanoparticles were spherical in shape. Moreover, the high agglomeration of the biosynthesized AgNPs was possibly induced by dehydration exerted during the preparation of samples for SEM analysis.[34] In the EDX spectrum, the strong peak at 3 keV was due to the presence of the silver element. Carbon and oxygen were also detected in the spectrum, which were associated with the organic compounds of the leaf extract on the surface of Cp-AgNPs and play an important role in the reduction and stability of biosynthesized Cp-AgNPs.[35]

Antioxidant Activity Using DPPH and ABTS Assay. The in vitro antioxidant activity of the aqueous leaf extract of *C. prophetarum* and Cp-AgNPs was determined using DPPH and ABTS assays. From the analysis, we can conclude that the scavenging effect of the aqueous leaf extract and Cp-AgNPs on DPPH (Figure 6A) and ABTS radicals (Figure 6B) was

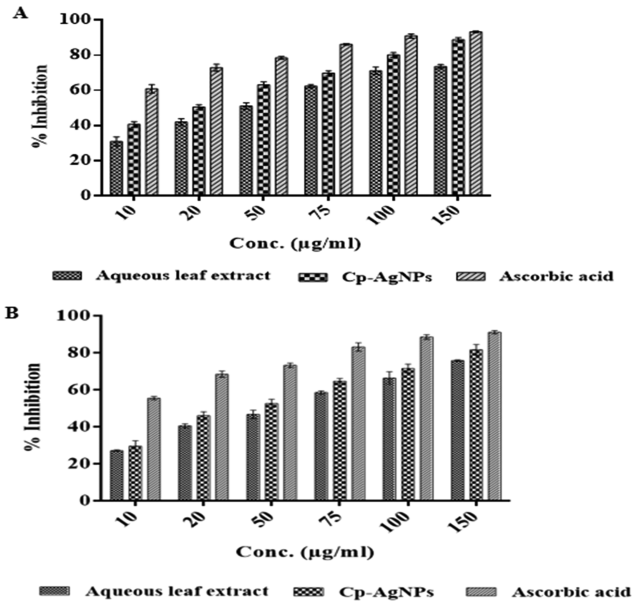

Figure 6. Free radical scavenging activity of different concentrations of the aqueous leaf extract of *C. prophetarum* and Cp-AgNPs using (A) DPPH scavenging effect and (B) ABTS assay.

increased in a dose-dependent manner; ascorbic acid was used as a standard. It was found that the Cp-AgNPs have higher free radical inhibition percentage with IC_{50} values of 29.2 and 34.5 μg/mL as compared to the aqueous leaf extract with IC_{50} values of 46.6 and 50 μg/mL using DPPH and ABTS, respectively.

The neutral and cationic radical quenching ability of the nanoparticles was assayed, which showed the capability of the Cp-AgNPs with stable neutral radicals obtained from DPPH and free cationic radicals from ABTS. Both applied tests presented different aspects of the antioxidative mechanism. While the DPPH assay shows the capacity of silver

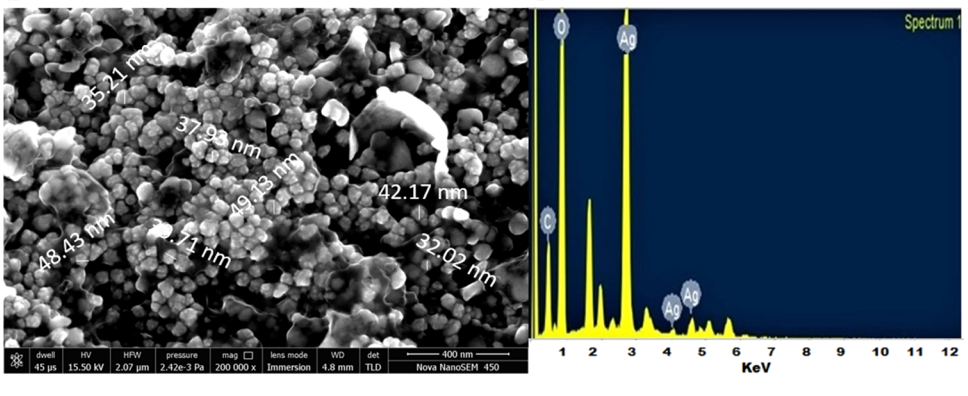

Figure 5. Electron microscopy study: (A) SEM analysis and (B) EDX spectra of Cp-AgNPs.

https://dx.doi.org/10.1021/acsomega.0c00155
ACS Omega 2020, 5, 5520−5528

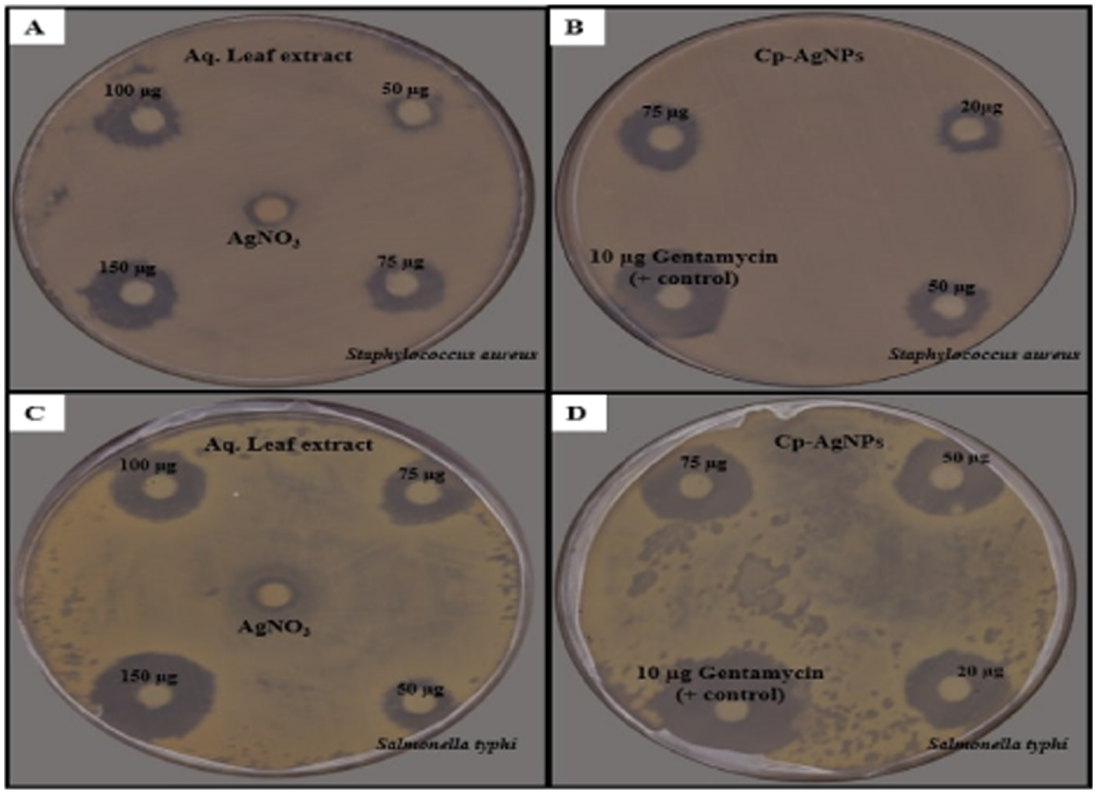

Figure 7. Bactericidal activity of different concentrations of (A) aqueous extract and (B) Cp-AgNPs against *S. aureus* and (C) aqueous extract and (D) Cp-AgNPs against *S. typhi*.

nanoparticles to transfer electrons to neutralize the free radicals of unstable DPPH in the reaction medium,[36] the ABTS assay determines the cationic free radical scavenging activity involving both electron and hydrogen transfer mechanisms.[37]

Antibacterial Activity Using Disc Diffusion Assay. The antibacterial activity of the aqueous leaf extract of *C. prophetarum* and biosynthesized Cp-AgNPs was checked by the disc diffusion method against *S. aureus* (Gram-positive) and *S. typhi* (Gram-negative) bacteria, as shown in Figure 7. Cp-AgNPs showed high antibacterial activity in terms of zone of inhibition against *S. aureus* and *S. typhi* (Figure 7B,D) when compared to the aqueous leaf extract of *C. prophetarum* (Figure 7 A,C). The maximum zone of inhibition at the highest concentration of Cp-AgNPs was 18 and 20 mm against *S. aureus* (Figure 7B) and *S. typhi*, respectively (Figure 7D). Cp-AgNPs showed higher antibacterial activity against *S. typhi* as compared to *S. aureus* in a dose-dependent manner, as shown in Table 2.

The zone of inhibition on all bacterial strains was measured after 24 h of incubation at 37 °C. The aqueous leaf extract showed significant antibacterial activity and was found to be lower when applied alone as compared with Cp-AgNPs (Table 2). Comparative antibacterial activities using the leaf extract of *Artemisia vulgaris* also resulted in similar findings.[36] The diameter of the inhibition zone is larger for *S. typhi* as compared to *S. aureus*. The antibacterial activity of AgNPs is more pronounced in the case of the Gram-negative bacteria as reported.[18] This minor difference can be due to the difference in the composition of their cell wall, as the cell membrane of Gram-negative bacteria consists of a single layer of peptidoglycan, while multiple layers of peptidoglycan are present in the membrane of Gram-positive bacteria, which

Table 2. Zone of Inhibition of Gram-Positive and Gram-Negative Bacteria Using Different Concentrations of the Aqueous Leaf Extract and Cp-AgNPs

test sample	conc. (µg/mL)	zone of inhibition *S. aureus* (mm)	zone of inhibition *S. typhi* (mm)
aqueous leaf extract	50	10 ± 0.5	12 ± 0.2
	75	12 ± 0.3	14 ± 0.4
	100	13 ± 0.6	15 ± 0.5
	150	15 ± 0.4	18 ± 0.7
biosynthesized Cp-AgNPs	20	11 ± 0.4	15 ± 0.2
	50	14 ± 0.3	17 ± 0.5
	75	18 ± 0.4	20 ± 0.6
DMSO	10	21 ± 0.5	24 ± 0.4

makes them more rigid.[38] The silver ions from nanoparticles are attracted by the negative charge of the bacterial cell wall, and when they experience some electrostatic attraction toward the bacterial cell wall, they will move and get attached to the cell wall and lead to a change in the composition of the cell wall by affecting its permeability.[39] The DNA of micro-organisms loses its replication ability and also the expression of ribosome subunit proteins as well as other cellular proteins, and most of the enzymes essential for ATP production become inactivated upon treatment with Ag^+ ions.[40]

Assessment of Antiproliferative Activity on Cancer Cell Lines. To check the antiproliferative activity of the green-synthesized Cp-AgNPs, different concentrations of nanoparticles were added to cancer cell lines, such as A549, MDA-MB-231, HepG2, and MCF-7, and they were incubated for 24 h. The MTT assay result shows that there is a gradual decrease in cell viability with increasing concentration of Cp-AgNPs (Figure 8). The IC_{50} value of Cp-AgNPs for A549,

https://dx.doi.org/10.1021/acsomega.0c00155
ACS Omega 2020, 5, 5520−5528

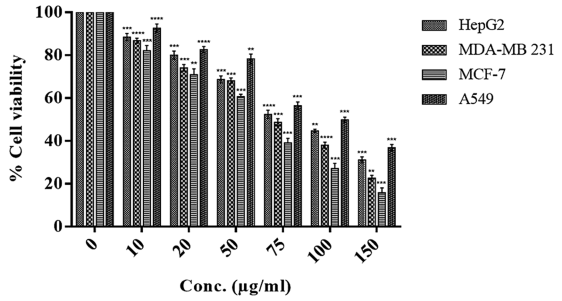

Figure 8. Effect of different concentrations of Cp-AgNPs on the viability of human cancer cell lines. One-way analysis of variance (ANOVA) multiple comparisons; ****P-value signifies < 0.0001, ***P-value signifies < 0.001, **P-value signifies < 0.01, and *P-value signifies < 0.05.

MDA-MB-231, HepG2, and MCF-7 was calculated to be 105.8, 81.1, 94.2, and 65.6 μg/mL, respectively. At the IC_{50} concentration of Cp-AgNPs, the morphology of the cells was observed under an inverted microscope (Figure 9).

Depending on the results of the antiproliferative activity analysis, we may conclude that the biosynthesized AgNPs are more toxic toward MCF-7 as compared to the MDA-MB-231, HepG2, and A549 cells, as shown in Figure 8. Silver nanoparticles synthesized using the leaf extract of *A. vulgaris* also showed an IC_{50} value close to 60 μg/mL for MCF-7 cells.[36] Our results are also in agreement with the effectiveness of the aqueous leaf extract of *C. sativus* against MCF-7 cells.[41] Methanolic leaf extract of *T. officinale* also exhibited enhanced activity against MCF-7 cell lines.[32] The present work is the first comparative study that investigates the cell viability of *C. prophetarum* leaf extract-mediated biosynthesized AgNPs against different cancer cell lines. Due to the enhanced cellular uptake and retention of NPs, the Cp-AgNPs showed a difference in cytotoxicity toward different cell lines. This is because the NPs can enter the cells via endocytosis due to their small size and are not subjected to efflux by *P*-glycoprotein.[42]

CONCLUSIONS

The synthesis of AgNPs using *C. prophetarum* through a green chemistry approach with several advantages such as an economic, efficient, and ecofriendly process, which is also energy-efficient and cost-effective, results in healthier workplaces and communities, protecting human health and the environment, leading to less waste and safer products. The potentially active phytoconstituents involved in the plant-mediated synthesis of nanoparticles are biocompatible for a wide range of biomedical applications. Additionally, the nanoparticles were studied to show their antibacterial activity against Gram-positive and Gram-negative bacteria and antiproliferative effects on different human cancer cell lines, which were A549, MDA-MB-231, HepG2, and MCF-7, in a dose-dependent manner. Thus, this report adds another feature to the medicinal hub plant *C. prophetarum*, i.e., its ability to successfully formulate AgNPs, which could be used effectively for their antibacterial and antiproliferative properties.

MATERIALS AND METHODS

Materials. Silver nitrate ($AgNO_3$), Muller Hilton Agar, 3-(4,5-dimethylthiazol-2-yl)-2,5-diphenyltetrazolium bromide (MTT), 2,2-diphenyl-1-picrylhydrazyl (DPPH), 2,2′-azino-bis(3-ethylbenzothiazoline-6-sulfonic acid) (ABTS), and dimethyl sulfoxide (DMSO) were procured from HiMedia. All

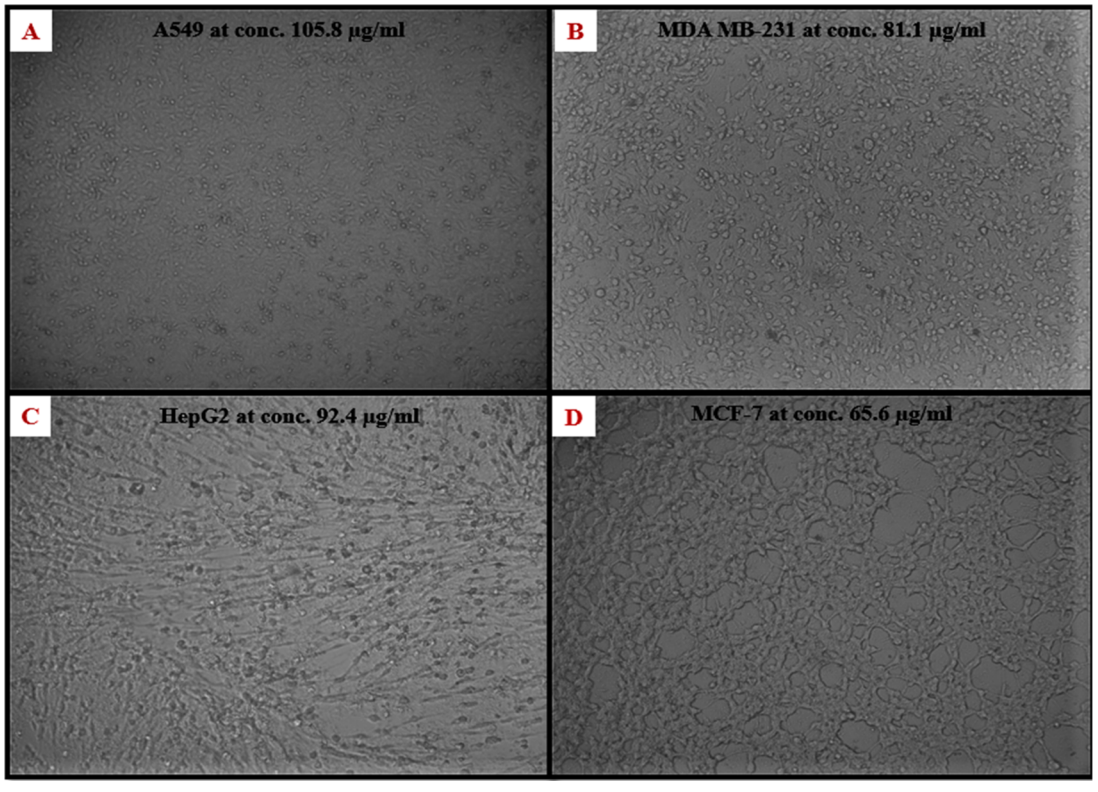

Figure 9. Morphology at the IC_{50} concentration of Cp-AgNPs of cancer cell lines (A) A549, (B) MDA-MB-231, (C) HepG2, and (D) MCF-7.

https://dx.doi.org/10.1021/acsomega.0c00155
ACS Omega 2020, 5, 5520−5528

other chemicals used were of analytical grade and high purity and were procured from reputed firms.

Collection of Plant Material and Preparation of Extract. Leaves of *C. prophetarum* were collected from the Central University of Rajasthan, Kishangarh, Ajmer. The specimen sample was taxonomically identified and authenticated by the Department of Botany, Rajasthan University, where a voucher specimen was deposited (authentication no. RUBL No. 211677). The leaves were washed thoroughly with distilled water and allowed to dry in the shade at room temperature. The dried leaves were crushed using an electric lab blender to make fine powder. For 25 g of leaf powder, 250 mL of distilled water was added, and the mixture was heated at 80 °C for 3 h with continuous stirring, and the resultant extract was then filtered through Whatman filter paper no. 1. The extract was stored at 4 °C until further use.

Preliminary Phytochemical Analysis. Preliminary phytochemical analysis was performed to determine various phytoconstituents present in the freshly prepared leaf extracts of *C. prophetarum,* such as phenol, triterpenoids, tannins, flavonoids, saponins, and alkaloids using standard phytochemical procedures followed by Cyril et al.[43]

Green Synthesis of Silver Nanoparticles. For the green synthesis of silver nanoparticles, we used the aqueous leaf extract of *C. prophetarum* prepared in the previous step. For this, 10 mL of leaf extract was added to 90 mL of 1 mM aqueous silver nitrate solution, followed by heating at 80 °C for 3 h with constant stirring. The formation of the AgNPs was preliminarily detected by the change in color from yellow to dark brown. The green-synthesized nanoparticles were separated using centrifugation at 15,000 × *g* for 20 min. This process was repeated thrice to get rid of free silver associated with Cp-AgNPs. The final green-synthesized silver nanoparticles were denoted as Cp-AgNPs, which were freeze-dried and then stored at 4 °C until further use.

Characterization of Silver Nanoparticles. *UV−vis Spectroscopic Measurements.* UV−vis spectra were recorded to check the reduction of silver nitrate with *C. prophetarum* leaf extract using an HMG Labtech SPECTROstar Nano in the range of 220−700 and 1 nm resolution.

Particle Size, PDI, and ζ-Potential Measurements. The average hydrodynamic particle size distribution, PDI, and ζ-potential of the nanoparticles were measured using a Zetasizer nanoZS (Malvern Instruments, Malvern, U.K.) by the dynamic light scattering (DLS) technique. The size measurements were carried out at 25 °C, adjusting the light scattering angle at 90°. The surface charge (ζ-potential) of the Cp-AgNPs was measured using an electrophoretic cell under an electric field. The sample was prepared by diluting the nanoparticles with MilliQ water and ultrasonicating for 5 min to obtain a well-dispersed suspension.

Functional Group Analysis by FTIR Measurements. The functional groups present in the phytoconstituents responsible for the reduction and capping of Cp-AgNPs were analyzed with an FTIR spectrophotometer (PerkinElmer Spectrum Version 10.4.00, M/s PerkinElmer Co., Waltham, Massachusetts) using the KBr pellet method. The scanning range of the FTIR spectrophotometer was 4000−400 $cm^{-1}$with a spectral resolution of 1 cm^{-1}.

XRD Analysis. XRD was used to investigate the phase and crystalline structure of the biosynthesized Cp-AgNPs. The analysis was done on an X-ray diffractometer (PANalytical-Empyrean) using Cu Kα radiation with a wavelength of 1.540 A° at 40 kV and 30 mA, and a scanning rate of 0.02 cm^{-1} in the region of 2θ ranging between 30 and 90°.

FESEM and Energy-Dispersive X-ray Analysis (EDAX) of Cp-AgNPs. FESEM integrated with EDX was used to examine the surface morphology, size, and atomic content of metals in biosynthesized Cp-AgNPs. The surface morphology of the Cp-AgNPs was measured using a scanning electron microscope (EVO 18, ZEISS) at a magnification of 10 000×. The samples were fixed on the tubular aluminum stub with double-sided tape. The stub-supported samples were coated with gold. Finally, the gold-coated samples were placed under the microscope to observe the morphology.

Antioxidant Activity. *DPPH Free Radical Scavenging Assay.* The antioxidant activity of the aqueous leaf extract was evaluated using the DPPH radical scavenging method.[44] Briefly, 100 μL of various concentrations of Cp-AgNPs, plant extract, and standard (ascorbic acid) (10, 20, 50, 75, 100, and 150 μg/mL) were mixed with 100 μL of DPPH (0.1 mM in 80% ethanol) and incubated in the dark for 30 min at room temperature (RT). The absorbance of the reaction mixtures was measured using a BMG Labtech spectrophotometer at 517 nm against a blank (80% ethanol). DPPH free radical scavenging activity percentage was calculated using the formula given below

$$\text{DPPH radical scavenging ability}(\%) = [(\text{Abs of control} - \text{Abs of sample})/\text{Abs of control}] \times 100$$

The IC_{50} values of the extract and nanoparticles were calculated from the graph using the equation $Y = mX$ and the linear regression coefficient.

ABTS Free Radical Scavenging Assay. The ABTS radical scavenging activity of different concentrations of the aqueous leaf extract and Cp-AgNPs was estimated by a standard protocol.[45] The stock solution of ABTS was prepared by mixing ABTS (7 mM) with potassium persulfate (2.45 mM), and then the mixture was incubated at RT in the dark for 16 h. After that, the working solution was obtained by diluting the stock solution with methanol to obtain an absorbance of around 0.85 ± 0.20 at 734 nm. Then, 20 μL of various concentrations (10, 20, 50, 75, 100 and 150 μg/mL) of the aqueous leaf extract and Cp-AgNPs were added to 180 μL of ABTS working solution. The mixture was left for 30 min at room temperature and the absorbance was measured using a BMG Labtech spectrophotometer at 734 nm. Ascorbic acid was taken as a standard. ABTS free radical scavenging percentage activity was calculated using the following formula

$$\text{ABTS radical scavenging}(\%) = [(\text{Abs of control} - \text{Abs of sample})/\text{Abs of control}] \times 100$$

Antibacterial Activity Using the Disc Diffusion Method. The antibacterial activity of the aqueous leaf extract of *C. prophetarum* and biosynthesized Cp-AgNPs was determined using the disc diffusion method.[46] A bacterial inoculum suspension was spread uniformly on solidified Muller−Hinton Agar (MHA) using a sterile swab. The bacterial strains used in this study were Gram-positive *Staphylococcus aureus* (MTCC96) and Gram-negative *S. typhi* (ATCC13076). A fixed volume of about 25 μL having different

https://dx.doi.org/10.1021/acsomega.0c00155
ACS Omega 2020, 5, 5520−5528

concentrations of the aqueous leaf extract (50, 75, 100, and 150 μg/mL) and green-synthesized Cp-AgNPs (20, 50, and 75 μg/mL) was added into different discs and placed in Petri plates for incubation at 37 °C for 24 h. The obtained zones of inhibition were measured in millimeters. A disc loaded with 10 μg of gentamycin was used as the positive control and DMSO was used as the negative control.

Culturing of Cell Lines. Different types of cancer cell lines, such as a lung cancer cell line (A549), breast cancer cell lines (MDA-MB-231 and MCF-7), and a hepatic cancer cell line (HepG2), were used for assessment of the proliferative effect of green-synthesized Cp-AgNPs. Dulbecco's modified Eagle's medium (DMEM) supplemented with 10% fetal bovine serum (FBS) and 1% penicillin−streptomycin was used to subculture the cell lines in a CO_2 incubator with 5% CO_2. Cells were counted, and the cell viability was checked by trypan blue using a hemocytometer. The cells were seeded at 1×10^4 in a 96-well plate for performing MTT assay for 24 h at 37 °C in the CO_2 incubator.

Assessment of Antiproliferative Activity on Cancer Cell Lines. A549, MDA-MB-231, HepG2, and MCF-7 cell lines were treated with different concentrations (10, 20, 50, 75, 100, and 150 μg/mL) of biosynthesized Cp-AgNPs. The dilutions were prepared in DMSO. After treatment, the cells were incubated for 24 h in the CO_2 incubator. After 24 h, the morphology of the cells was observed under a microscope, and then, 20 μL of the MTT reagent (5 mg/mL) was added and incubated for 4 h at 37 °C. After incubation, the formazan produced was solubilized by the addition of 100 μL of DMSO. The absorbance was measured at 570 nm using a 96-well plate reader, and the cell viability was calculated as follows

$$[\text{mean Abs(treated sample)} - \text{blank Abs}]/[\text{mean Abs(control)} - \text{blank Abs}] \times 100$$

Statistical Analysis. Data were analyzed in a grouped analysis by ANOVA using GraphPad Prism software. P-value < 0.05 was considered as a significant level between treated and control sets. The results were denoted as mean ± standard deviation of three experiments.

AUTHOR INFORMATION

Corresponding Author

Kiran Kumar Tejavath − *Department of Biochemistry, School of Life Sciences, Central University of Rajasthan, Ajmer 305817, Rajasthan, India;* orcid.org/0000-0001-7876-421X; Phone: +91 7725908348; Email: kirankumar@curaj.ac.in

Authors

Hemlata − *Department of Biochemistry, School of Life Sciences, Central University of Rajasthan, Ajmer 305817, Rajasthan, India*

Prem Raj Meena − *Department of Microbiology, School of Life Sciences, Central University of Rajasthan, Ajmer 305817, Rajasthan, India*

Arvind Pratap Singh − *Department of Microbiology, School of Life Sciences, Central University of Rajasthan, Ajmer 305817, Rajasthan, India*

Complete contact information is available at: https://pubs.acs.org/10.1021/acsomega.0c00155

Notes

The authors declare no competing financial interest.

ACKNOWLEDGMENTS

The authors would like to acknowledge the financial support received from the Department of Science and Technology (SERB/EEQ/2016/000696) and University Grants Commission (UGC-RGNF) for the award of Junior Research Fellowship. The authors would also like to acknowledge the Department of Physics, Central University of Rajasthan, Ajmer, India, for XRD analysis; Material Research Centre, Malviya National Institute of Technology, Jaipur, for FTIR analysis; and AIIMS, New Delhi, India, for SEM and EDAX analysis.

REFERENCES

(1) Erci, F.; Cakir-Koc, R.; Isildak, I. Green synthesis of silver nanoparticles using Thymbra spicata L. var. spicata (zahter) aqueous leaf extract and evaluation of their morphology-dependent antibacterial and cytotoxic activity. *Artif. Cells, Nanomed., Biotechnol.* **2018**, *46*, 150−158.

(2) Tanase, C.; Berta, L.; Coman, N. A.; Rosca, I.; Man, A.; Toma, F.; Mocan, A.; Jakab-Farkas, L.; Biro, D.; Mare, A. Investigation of In Vitro Antioxidant and Antibacterial Potential of Silver Nanoparticles Obtained by Biosynthesis Using Beech Bark Extract. *Antioxidants* **2019**, *8*, No. 459.

(3) Behboodi, S.; Baghbani-Arani, F.; Abdalan, S.; Sadat Shandiz, S. A. Green Engineered Biomolecule-Capped Silver Nanoparticles Fabricated from Cichorium intybus Extract: In Vitro Assessment on Apoptosis Properties Toward Human Breast Cancer (MCF-7) Cells. *Biol. Trace Elem. Res.* **2019**, *187*, 392−402.

(4) Gengan, R.; Anand, K.; Phulukdaree, A.; Chuturgoon, A. A549 lung cell line activity of biosynthesized silver nanoparticles using Albizia adianthifolia leaf. *Colloids Surf., B* **2013**, *105*, 87−91.

(5) Rajan, R.; Chandran, K.; Harper, S. L.; Yun, S.-I.; Kalaichelvan, P. T. Plant extract synthesized silver nanoparticles: an ongoing source of novel biocompatible materials. *Ind. Crops Prod.* **2015**, *70*, 356−373.

(6) Ahn, E. Y.; Jin, H.; Park, Y. Assessing the antioxidant, cytotoxic, apoptotic and wound healing properties of silver nanoparticles green-synthesized by plant extracts. *Mater. Sci. Eng., C* **2019**, *101*, 204−216.

(7) Fahimirad, S.; Ajalloueian, F.; Ghorbanpour, M. Synthesis and therapeutic potential of silver nanomaterials derived from plant extracts. *Ecotoxicol. Environ. Saf.* **2019**, *168*, 260−278.

(8) Haggag, E. G.; Elshamy, A. M.; Rabeh, M. A.; Gabr, N. M.; Salem, M.; Youssif, K. A.; Samir, A.; Bin Muhsinah, A.; Alsayari, A.; Abdelmohsen, U. R. Antiviral potential of green synthesized silver nanoparticles of Lampranthus coccineus and Malephora lutea. *Int. J. Nanomed.* **2019**, *14*, 6217−6229.

(9) Totaro, P.; Rambaldini, M. Efficacy of antimicrobial activity of slow release silver nanoparticles dressing in post-cardiac surgery mediastinitis. *Interact. Cardiovasc. Thorac. Surg.* **2009**, *8*, 153−154.

(10) Nee, M. The domestication ofcucurbita (cucurbitaceae). *Econ. Bot.* **1990**, *44*, 56.

(11) Alsayari, A.; Kopel, L.; Ahmed, M. S.; Soliman, H. S. M.; Annadurai, S.; Halaweish, F. T. Isolation of anticancer constituents from Cucumis prophetarum var. prophetarum through bioassay-guided fractionation. *BMC Complementary Altern. Med.* **2018**, *18*, No. 274.

(12) Ayyad, S. E.; Abdel-Lateff, A.; Basaif, S. A.; Shier, T. Cucurbitacins-type triterpene with potent activity on mouse embryonic fibroblast from Cucumis prophetarum, cucurbitaceae. *Pharmacogn. Res.* **2011**, *3*, 189−93.

(13) Kavishankar, G.; Lakshmidevi, N. Anti-diabetic effect of a novel N-Trisaccharide isolated from Cucumis prophetarum on Streptozotocin−nicotinamide induced type 2 diabetic rats. *Phytomedicine* **2014**, *21*, 624−630.

(14) Senthil, V.; Ramasamy, P.; Elaiyaraja, C.; Elizabeth, A. R. Some phytochemical prosperities affected by the infection of leaf spot disease of *Cucumis sativus* (Linnaeus) caused by Penicillium notatum. *Afr. J. Basic Appl. Sci.* **2010**, *2*, 64−70.

https://dx.doi.org/10.1021/acsomega.0c00155
ACS Omega 2020, 5, 5520−5528

(15) Babulreddy, N.; Sahoo, S. P.; Ramachandran, S.; Dhanaraju, M. Anti-hyperglycemic activity of *Cucumis Melo* Leaf extracts in Streptozotocin induced Hyperglycemia in Rats. *Int. J. Pharm. Res. Allied Sci.* **2013**, *2*, 22−27.
(16) Jha, A. K.; Prasad, K.; Prasad, K.; Kulkarni, A. R. Plant system: nature's nanofactory. *Colloids Surf., B* **2009**, *73*, 219−223.
(17) Saratale, R. G.; Benelli, G.; Kumar, G.; Kim, D. S.; Saratale, G. D. Bio-fabrication of silver nanoparticles using the leaf extract of an ancient herbal medicine, dandelion (*Taraxacum officinale*), evaluation of their antioxidant, anticancer potential, and antimicrobial activity against phytopathogens. *Environ. Sci. Pollut. Res.* **2018**, *25*, 10392−10406.
(18) Bilal, M.; Rasheed, T.; Iqbal, H. M.; Li, C.; Hu, H.; Zhang, X. Development of silver nanoparticles loaded chitosan-alginate constructs with biomedical potentialities. *Int. J. Biol. Macromol.* **2017**, *105*, 393−400.
(19) Cervantes, B.; Arana, L.; Murillo-Cuesta, S.; Bruno, M.; Alkorta, I.; Varela-Nieto, I. Solid Lipid Nanoparticles Loaded with Glucocorticoids Protect Auditory Cells from Cisplatin-Induced Ototoxicity. *J. Clin. Med.* **2019**, *8*, No. 1464.
(20) Mohammed, A. E.; Bin Baz, F. F.; Albrahim, J. S. Calligonum comosum and Fusarium sp. extracts as bio-mediator in silver nanoparticles formation: characterization, antioxidant and antibacterial capability. *3 Biotech* **2018**, *8*, No. 72.
(21) Mariadoss, A. V. A.; Ramachandran, V.; Shalini, V.; Agilan, B.; Franklin, J. H.; Sanjay, K.; Alaa, Y. G.; Tawfiq, M. A.; Ernest, D. Green synthesis, characterization and antibacterial activity of silver nanoparticles by Malus domestica and its cytotoxic effect on (MCF-7) cell line. *Microb. Pathog.* **2019**, *135*, No. 103609.
(22) He, Y.; Wei, F.; Ma, Z.; Zhang, H.; Yang, Q.; Yao, B.; Huang, Z.; Li, J.; Zeng, C.; Zhang, Q. Green synthesis of silver nanoparticles using seed extract of Alpinia katsumadai, and their antioxidant, cytotoxicity, and antibacterial activities. *RSC Adv.* **2017**, *7*, 39842−39851.
(23) Bilal, M.; Zhao, Y.; Rasheed, T.; Ahmed, I.; Hassan, S. T.; Nawaz, M. Z.; Iqbal, H. Biogenic Nanoparticle-Chitosan Conjugates with Antimicrobial, Antibiofilm, and Anticancer Potentialities: Development and Characterization. *Int. J. Environ. Res. Public Health* **2019**, *16*, No. 598.
(24) Qais, F. A.; Shafiq, A.; Khan, H. M.; Husain, F. M.; Khan, R. A.; Alenazi, B.; Alsalme, A.; Ahmad, I. Antibacterial Effect of Silver Nanoparticles Synthesized Using *Murraya koenigii* (L.) against Multidrug-Resistant Pathogens. *Bioinorg. Chem. Appl.* **2019**, *2019*, No. 4649506.
(25) Mickymaray, S. One-step Synthesis of Silver Nanoparticles Using Saudi Arabian Desert Seasonal Plant Sisymbrium irio and Antibacterial Activity Against Multidrug-Resistant Bacterial Strains. *Biomolecules* **2019**, *9*, No. 662.
(26) Kumari, R.; Saini, A. K.; Kumar, A.; Saini, R. V. Apoptosis induction in lung and prostate cancer cells through silver nanoparticles synthesized from Pinus roxburghii bioactive fraction. *JBIC, J. Biol. Inorg. Chem.* **2019**, *63*, 1−15.
(27) Rodríguez-León, E.; Rodríguez-Vázquez, B. E.; Martínez-Higuera, A.; Rodríguez-Beas, C.; Larios-Rodríguez, E.; Navarro, R. E.; López-Esparza, R.; Iñiguez-Palomares, R. A. Synthesis of Gold Nanoparticles Using Mimosa tenuiflora Extract, Assessments of Cytotoxicity, Cellular Uptake, and Catalysis. *Nanoscale Res. Lett.* **2019**, *14*, No. 334.
(28) Rasheed, T.; Bilal, M.; Li, C.; Nabeel, F.; Khalid, M.; Iqbal, H. M. Catalytic potential of bio-synthesized silver nanoparticles using *Convolvulusarvensis* extract for the degradation of environmental pollutants. *J. Photochem. Photobiol., B* **2018**, *181*, 44−52.
(29) Bhuvaneswari, R.; Xavier, R. J.; Arumugam, M. Facile synthesis of multifunctional silver nanoparticles using mangrove plant *Excoecaria agallocha* L. for its antibacterial, antioxidant and cytotoxic effects. *J. Parasit. Dis.* **2017**, *41*, 180−187.
(30) B Aziz, S.; Hussein, G.; Brza, M.; J Mohammed, S.; T Abdulwahid, R.; Raza Saeed, S.; Hassanzadeh, A. Fabrication of Interconnected Plasmonic Spherical Silver Nanoparticles with Enhanced Localized Surface Plasmon Resonance (LSPR) Peaks Using Quince Leaf Extract Solution. *Nanomaterials* **2019**, *9*, No. 1557.
(31) Jeeva, K.; Thiyagarajan, M.; Elangovan, V.; Geetha, N.; Venkatachalam, P. Caesalpinia coriaria leaf extracts mediated biosynthesis of metallic silver nanoparticles and their antibacterial activity against clinically isolated pathogens. *Ind. Crops Prod.* **2014**, *52*, 714−720.
(32) Rasheed, T.; Bilal, M.; Li, C.; Iqbal, H. Biomedical potentialities of *Taraxacum officinale*-based nanoparticles biosynthesized using methanolic leaf extract. *Curr. Pharm. Biotechnol.* **2018**, *18*, 1116−1123.
(33) Ajayi, E.; Afolayan, A. Green synthesis, characterization and biological activities of silver nanoparticles from alkalinized Cymbopogon citratus Stapf. *Adv. Nat. Sci.: Nanosci. Nanotechnol.* **2017**, *8*, No. 015017.
(34) Sigamoney, M.; Shaik, S.; Govender, P.; Krishna, S. B. N.; Sershen. African leafy vegetables as bio-factories for silver nanoparticles: A case study on Amaranthus dubius C Mart. Ex Thell. *S. Afr. J. Bot.* **2016**, *103*, 230−240.
(35) Jagtap, U. B.; Bapat, V. A. Green synthesis of silver nanoparticles using Artocarpus heterophyllus Lam. seed extract and its antibacterial activity. *Ind. Crops Prod.* **2013**, *46*, 132−137.
(36) Rasheed, T.; Bilal, M.; Iqbal, H. M.; Li, C. Green biosynthesis of silver nanoparticles using leaves extract of *Artemisia vulgaris* and their potential biomedical applications. *Colloids Surf., B* **2017**, *158*, 408−415.
(37) Sowinska, M.; Morawiak, M.; Bochynska-Czyz, M.; Lipkowski, A. W.; Zieminska, E.; Zablocka, B.; Urbanczyk-Lipkowska, Z. Molecular Antioxidant Properties and In Vitro Cell Toxicity of the p-Aminobenzoic Acid (PABA) Functionalized Peptide Dendrimers. *Biomolecules* **2019**, *9*, No. 89.
(38) Netai, M.-M.; Moyo Joyce, N.; Stephen, N.; Musekiwa, C. Synthesis of silver nanoparticles using wild *Cucumis anguria*: Characterization and antibacterial activity. *Afr. J. Biotechnol.* **2017**, *16*, 1911−1921.
(39) Ahmed, S.; Ahmad, M.; Swami, B. L.; Ikram, S. A review on plants extract mediated synthesis of silver nanoparticles for antimicrobial applications: A green expertise. *J. Adv. Res.* **2016**, *7*, 17−28.
(40) Franci, G.; Falanga, A.; Galdiero, S.; Palomba, L.; Rai, M.; Morelli, G.; Galdiero, M. Silver nanoparticles as potential antibacterial agents. *Molecules* **2015**, *20*, 8856−8874.
(41) Tuama, A. A.; Mohammed, A. A. Phytochemical screening and in vitro antibacterial and anticancer activities of the aqueous extract of *Cucumis sativus*. *Saudi J. Biol. Sci.* **2019**, *26*, 600−604.
(42) Satpathy, S.; Patra, A.; Ahirwar, B.; Delwar Hussain, M. Antioxidant and anticancer activities of green synthesized silver nanoparticles using aqueous extract of tubers of Pueraria tuberosa. *Artif. Cells, Nanomed., Biotechnol.* **2018**, *46*, S71−S85.
(43) Cyril, N.; George, J. B.; Joseph, L.; Raghavamenon, A. C. Assessment of antioxidant, antibacterial and anti-proliferative (lung cancer cell line A549) activities of green synthesized silver nanoparticles from *Derris trifoliata* **2019**, *8* 297 308. DOI: 10.1039/c8tx00323h.
(44) Cheng, Z.; Moore, J.; Yu, L. High-throughput relative DPPH radical scavenging capacity assay. *J. Agric. Food Chem.* **2006**, *54*, 7429−7436.
(45) Re, R.; Pellegrini, N.; Proteggente, A.; Pannala, A.; Yang, M.; Rice-Evans, C. Antioxidant activity applying an improved ABTS radical cation decolorization assay. *Free Radicals Biol. Med.* **1999**, *26*, 1231−1237.
(46) Bauer, A.; Kirby, W.; Sherris, J. C.; Turck, M. Antibiotic susceptibility testing by a standardized single disk method. *Am. J. Clin. Pathol.* **1966**, *45*, 493−496.

https://dx.doi.org/10.1021/acsomega.0c00155
ACS Omega 2020, 5, 5520−5528